UNIVERSITY OF CALIFORNIA

Los Angeles

An Investigation into Cell-Type Vulnerability for Formation of Alpha-Synuclein Aggregates

A thesis submitted in partial satisfaction

of the requirements for the degree Master of Science

in Physiological Science

by

Scarlett Milena Ramos Rodriguez

2023

ABSTRACT OF THE THESIS

An Investigation into Cell-Type Vulnerability for Formation of Alpha-Synuclein Aggregates

by

Scarlett Milena Ramos Rodriguez

Master of Science in Physiological Science

University of California, Los Angeles, 2023

Professor William Zeiger, Co-Chair

Professor Elaine Yih-Nien Hsiao, Co-Chair

Parkinson's Disease (PD) is a common, disabling neurodegenerative disorder neuropathologically defined by the loss of dopaminergic neurons in the substantia nigra pars compacta (SNc) and the accumulation of intracellular Lewy body inclusions[7]. Lewy body inclusions are primarily composed of misfolded alpha-synuclein fibrils. Multiple lines of evidence from human autopsy studies and animal models suggest that misfolded α-Syn aggregates can be transferred between neurons, propagating α-Syn pathology throughout the brain in a prion-like manner. However, α-Syn pathology does not spread diffusely, but rather certain brain regions display a selective vulnerability to α-Syn aggregate formation. Levels of α-

Syn expression and anatomical connectivity partially explain the observed regional vulnerability, but additional factors must be involved as well. We hypothesized that certain types of neurons may be more likely to form α-Syn pathology than others. To investigate whether there is a cell type specific vulnerability for α-Syn aggregate formation, we used the pre-formed fibril (PFF) model of PD. Specifically, we injected PFFs directly into either the primary motor cortex or the dorsolateral striatum. We then used immunofluorescence staining to quantify pathological α-Syn aggregates and to co-localize these with markers for specific neuronal subpopulations. We found that injection of α-Syn PFFs leads to the local accumulation of pathological α-Syn aggregates. In both the cortex and dorsolateral striatum, non-somatically localized aggregates were more numerous than somatically localized aggregates. In the cortex, we observed somatic α-Syn aggregates colocalizing with excitatory neurons and inhibitory interneurons. A greater proportion of inhibitory interneurons colocalized with somatic α-Syn aggregates than excitatory neurons. Furthermore, in the dorsolateral striatum, both D1 and D2 medium spiny neurons (MSNs) colocalized with somatic α-Syn aggregates, with a higher proportion of D1 MSNs colocalizing with somatic α-Syn compared to D2 MSNs. These results suggest that there may be some mechanisms contributing to a cell-type vulnerability for α-Syn aggregate formation. Further research investigating these mechanisms may offer new approaches for therapeutic disease intervention in PD.

The thesis of Scarlett Milena Ramos Rodriguez is approved.

David L. Glanzman

Elaine Yih-Nien Hsiao, Committee Co-Chair

William Zeiger, Committee Co-Chair

University of California, Los Angeles

2023

DEDICATION

I would like to dedicate this thesis to my parents, Milena Enna Ramos Rodriguez and Albert Manzo Ramos. Without their endless love and sacrifices, this thesis would not have been possible. Dad, thank you for always knowing the right thing to say. Mom, thank you for your endless support. I love you both very much.

TABLE OF CONTENTS

LIST OF TABLE AND FIGURES

ACKNOWLEDGMENTS

I would like to thank my mentor, Dr. William Zeiger, for his endless patience and support in this journey. Your guidance has made me into the scientist I am today. Thank you for never giving up on me and teaching me that I am more than capable of achieving whatever I set my mind to. Through you, I have learned that I do belong. My time in the Zeiger Lab has been life changing. I will forever be grateful for you taking a chance on me and allowing me the opportunity to join your team. Through my time in the lab, I have grown both academically and personally, more than I could have ever imagined.

I would like to thank Callie Liu for her immense support. Without your mice colony expertise this project would not have been possible. Thank you for always lending an ear. Whether it was me troubleshooting experiments or life experiences, you have always been there for me. Your kindness and support mean the world to me. Hot pot and boba for life. We started our time in the lab as co-workers but leave as great friends.

Thank you Dr. Aye Theint Theint for all your support and guidance. Your mentorship and friendship are invaluable to me. Additionally, I would like to thank Brenda Vasquez and Dr. Baruc Campos for their help. You both are vital people to my graduate school experience. I will forever be grateful to the Zeiger Lab.

Thank you to my committee members Dr. Elaine Yih-Nien Hsiao and Dr. L. Glanzman for their assistance and feedback throughout this process.

Lastly, I would also like to thank Marisela Diaz Vasquez and Dr. Amy Rowat for their immense guidance and support throughout my graduate school journey. You both have been an influential aspect of my time at UCLA.

This project was made possible by the following grant: UCLA David Binder Research Fund.

INTRODUCTION

Parkinson's Disease (PD) is the second-most prevalent neurodegenerative disease[1] affecting over 1.9% of the population over 80 years old[2]. PD incidence is different by sex, with males being 1.5 times more likely to develop PD than females[3]. Most PD cases are classified as sporadic, with only about 15% being familial[4]. In the early stages of PD, patients often experience prominent motor symptoms, such as tremors, bradykinesia, and rigidity[5]. Many individuals also experience non-motor symptoms such as sleep disorders, orthostatic hypotension, and cognitive defects, some of which may even precede the onset of motor symptoms[5]. Approximately 80% of PD patients may progress to Parkinson's disease with dementia [PDD]) 10-20 years after diagnosis[6].

PD is neuropathologically defined by the loss of dopaminergic neurons in the substantia nigra pars compacta (SNc) in conjunction with the presence of Lewy body inclusions, including Lewy neurites and Lewy bodies[7]. Lewy body inclusions are primarily composed of misfolded alpha-synuclein (α-Syn)[7], which is encoded by the *SNCA* gene[5]. Endogenous α-Syn is primarily localized to the presynaptic terminals of neurons[8]. While the exact function of α-Syn remains debated, it is thought to influence processes at the synapses, such as dopamine metabolism, membrane remodeling, and neurotransmitter release[9]. Pathological α-Syn is thought to first misfold at presynaptic sites, aggregating into fibrils and forming lewy neurites, with Lewy bodies forming later in the soma of neurons[10]. While the loss of dopaminergic neurons in the SNc is likely responsible for many of the motor symptoms in PD, the mechanisms underlying the development of other PD symptoms, such as cognitive defects, remain incompletely understood. Likewise, while dopamine replacement therapies can provide some symptomatic relief of motor disabilities, there are no treatments that can alter the progression of PD[1] or the development of cognitive impairments and dementia.

It is hypothesized that misfolded α-Syn plays a vital role in the development of PD[1]. Findings from numerous cell and animal model studies have demonstrated the toxicity of α-

Syn[11]. In mice that were unilaterally injected with α-Syn PFFs at the striatum, Lewy body formation resulted in the degeneration of dopamine neurons[12]. Some hypotheses regarding the mechanisms behind α-Syn toxicity are obstructed transport between the endoplasmic reticulum (ER) and Golgi body, ER stress, reduction in the release of synaptic vesicles, and apoptosis[11].

A postmortem study conducted by Braak et al. found that the distribution of misfolded α-Syn pathology correlates with disease severity in patients with PD and follows a stereotypical anatomical distribution[13]. In the early stages of PD, misfolded α-Syn pathology is first observed in the dorsal motor nucleus of the glossopharyngeal and anterior olfactory nucleus[13]. α-Syn pathology is noted to then spread to regions such as the caudal raphe nuclei, gigantocellular reticular nucleus, and coeruleus-subcoeruleus complex[13]. In patients with moderate stages of PD, misfolded α-Syn pathology is present in the midbrain, including the substantia nigra, and in more advanced stages, α-Syn pathology is found in the basal ganglia and eventually neocortical areas[13].

In a clinical study conducted by Li, fetal mesencephalic dopaminergic neurons were transplanted into two individuals with PD[14]. After the individuals passed away due to causes unrelated to the grafting, a postmortem exam was conducted on the recipients[14]. Li and colleagues noted that α-Syn pathology was observed in the grafted neurons[14]. Together with Braak's findings, these results were critical to the generation of the hypothesis that misfolded α-Syn pathology may spread throughout the brain over time, being transferred between neurons along anatomically connected pathways, resulting in the misfolding of α-Syn in the recipient neuron[1]. This hypothesis is known as the prion-like hypothesis.

The prion-like hypothesis has been recapitulated in various PD models[1]. Luk and colleagues revolutionized the study of PD by demonstrating that the addition of recombinant α-Syn pre-formed fibrils (PFFs) to cultured cells overexpressing α-Syn resulted in the formation of α-Syn aggregates[15]. Volpicelli-Daley and others went on to demonstrate that the addition of α-Syn PFFs to primary neuronal cultures leads to the formation of Lewy-like aggregates[16]. In

mice, injection of α-Syn PFFs leads to the formation of aggregated α-Syn inclusions, which over time spread between brain regions with anatomical connectivity to the injection site[12]. This injection model also displays time-dependent neurodegeneration of dopaminergic neurons in the SNc, a pathological hallmark of PD[12]. Furthermore, α-Syn seeding propagation in anatomically connected regions has also been observed after the injection of α-Syn PFFs into the olfactory bulb (OB)[17] and pedunculopontine nucleus (PPN)[18]. This α-Syn propagation model has also been applied to other model organisms. For example, in rats, injection of α-Syn PFFs into the striatum leads to a time-dependent propagation of pathological α-Syn in interconnected brain regions[19]. Likewise, in marmosets, α-Syn PFFs injections into the caudate nucleus and putamen result in Lewy body inclusions in anatomically connected regions[20]. Ultimately, the administration of α-Syn PFFs in various injection sites and model systems strongly supports the prion-like hypothesis of PD pathogenesis.

Across human pathology studies and the rodent PFF model, it has become clear that certain brain regions exhibit selective vulnerability to the accumulation of α-Syn pathology[21]. In rodent studies, anatomical connectivity and endogenous α-Syn expression levels are critical determinants behind the spread of misfolded α-Syn[1]. However, these factors alone are not sufficient to explain all of the regional vulnerability to the formation of α-Syn pathology. Henrich and colleagues went on to determine the cholinergic input connectome of the pedunculopontine nucleus (PPN) region of mice injected with alpha-synuclein PFFs[18]. They then compared the input strength of various brain regions to the amount of α-Syn pathology seen 1, 6, and 12 weeks post-injection[18]. They concluded that the spread of α-Syn pathology is not solely determined by synaptic connectivity[18]. One possibility is that certain types of neurons are more likely to form α-Syn aggregates than others. Accumulation of α-Syn pathology is well documented in dopaminergic neurons of the SNc, but the cell types that accumulate α-Syn in other brain regions are less well studied.

As previously mentioned, accumulation of α-Syn pathology in the cortex has been linked to cognitive impairment in PD. There are two major classes of neurons in the cortex. The first class of neurons are glutamatergic excitatory projection neurons [22], which constitute about 80% of cortical neurons. The gene *CAMK2α* has been used as a marker for excitatory neurons[23]. Inhibitory GABAergic interneurons are the second major class of neurons found in the cortex[22], and they account for about 10-20% of cortical neurons[24]. GABAergic interneurons can be broken down into three subdivisions. The most common are interneurons expressing the Ca^{2+}-binding protein paravalbumin (PV), which makes up about 40% of inhibitory neurons[24]. The other major groups of interneurons are defined by the expression of somatostatin (SST) and 5HT3aR, with both classes accounting for about 30% of inhibitory neurons[24]. Little is known about the selective vulnerability of cortical neurons to the formation of α-Syn pathology. In one study, after injection of α-Syn PFFs into the striatum of mice, α-Syn pathology was observed predominantly colocalizing with excitatory neurons in the prefrontal cortex[25].

On the other hand, motor dysfunction in PD is strongly linked to α-Syn pathology in the striatum. The striatum is composed of three main classes of neurons[26]. Medium spiny neurons (MSNs) are inhibitory and compose about 95% of the neurons in the striatum[26]. MSNs are primarily classified into two subtypes[27], D1 dopamine receptor (DRD1) expressing MSNs (D1-MSNs) and D2 dopamine receptor (DRD2) expressing MSNs (D2-MSNs)[27]. The remaining 5% of neurons in the striatum are GABAergic and cholinergic interneurons[27]. D1 and D2 MSNs play distinct roles in the basal ganglia, forming the direct and indirect pathways, respectively[28].

Given that α-Syn expression levels and anatomical connectivity alone are insufficient to fully explain regional vulnerability in PD, we hypothesize that there may be a cell-type specific vulnerability for the formation of α-Syn aggregates that may differ across different brain regions. Here we tested this hypothesis directly. We used the PFF model of PD and injected recombinant PFFs directly into either the motor cortex or dorsolateral striatum of mice. We then aged mice to allow for the formation of α-Syn pathology and used immunofluorescence staining

to determine the distribution of α-Syn pathology across different subpopulations of neurons in the cortex and dorsal striatum.

This study addresses a critical question in the field of PD research: Is there a cell type-specific vulnerability to the formation of α-Syn aggregates? The findings from this study will provide novel information about the transmission of misfolded α-Syn, which is likely to have a critical role in the development and progression of PD[29]. Furthermore, this study may provide new therapeutic targets, for example, by designing drugs to block aggregate formation in a cell-specific manner.

Materials and Methods

Mouse Genotypes and Maintenance

In Aim 1 of this study, we used female and male WT C57BL/6J mice. For Aim 2 of this study, we used hemizygous Tg(Drd1a-tdTomato)6Calak/J transgenic mice (strain ID #016204, JAX Laboratories)[30]. This strain of mice expresses tdTomato specifically in D1-type medium spiny neurons (MSNs). Both female and male mice were used for experiments. They were maintained on a 12:12 light-dark cycle in the Brain Research Institute Vivarium. All procedures were carried out in accordance with the Institutional Animal Care and Use Committee (IACUC) at the University of California, Los Angeles (UCLA) guidelines.

Stereotaxic Injections of α-Syn PFFs

Mice were anesthetized with 4% isoflurane in an induction chamber, then transferred onto a motorized stereotactic frame (Neurostar) and maintained at ~ 2% isoflurane. The scalp was then shaved and sterilized with 3 alternating swipes of betadine and 70% alcohol. A small incision was made, and a few drops of lidocaine were placed on the skull. A burr hole was created at the injection location using a pneumatic dental drill. Experimental mice were unilaterally injected with 3 µL of 2.5 mg/ml α-Syn PFFs in the left hemisphere at the brain region of interest. Control mice received an injection of 3 µL of Dulbecco's phosphate-buffer saline (DPBS) in the same region. Injections were performed using a glass capillary nanoinjector with a rate of 50 nL per minute except for one WT C57BL/6J mice, which received an injection of α-Syn PFFs at a rate of 50 to 100 nL per minute. α-Syn fibrils were a gift from our collaborator Dr. Chao Peng. α-Syn PFFs generation is detailed in ref[31]. PFFs were sonicated freshly on the injection day.

Stereotaxic surgeries were performed on 10-week-old WT C57BL/6J mice. Injections were performed into the primary motor cortex, at the following approximate coordinates: +1.18 mm AP, -1.66 mm ML, +1.74 mm DV.

Hemizygous Tg(Drd1a-tdTomato)6Calak/J transgenic mice received stereotaxic surgery at 8-10 weeks old. Injections were performed into the dorsal striatum at the approximate following coordinates +0.50 mm AP, -1.96 mm ML, +3.75 mm DV.

The incision site was closed via simple interrupted sutures. All mice received subcutaneous injections of 100 µL of 0.2 mg/kg of dexamethasone and 100 µL of 5 mg/kg of carprofen on the day of surgery and for two days post-injection to reduce pain and inflammation.

Histology and Immunohistochemistry

Mice were deeply anesthetized with isoflurane and transcardially perfused with ice cold phosphate-buffered saline (PBS), followed by 4% paraformaldehyde (PFA) in PBS. Brains were then removed and post-fixed in 4% PFA in PBS for 24-28 hours. They were then rinsed 3 times for 10 minutes in PBS. A compresstome (Precisionary instruments) was used to make 50 µm thick coronal sections. The sections were collected in PBS and later transferred into a cryoprotectant solution consisting of 30% glycerol and 30% sucrose in PBS.

Free-floating Immunohistochemistry (IHC) was then conducted on sections of interest. Sections were rinsed at room temperature five times for 10 minutes in PBS. The sections were then blocked at room temperature in 3% FBS and 3% BSA in PBS for ~140 minutes. Sections were then incubated in an antibody solution (3% FBS and 3% BSA in PBS) with the desired dilutions for the primary antibodies of interest for three days at 4℃. Sections were then washed at room temperature in PBS and incubated with secondary antibodies diluted in 3% FBS and 3% BSA in PBS at 4°C for ~24 hours. Sections were then rinsed at room temperature three times for 10 minutes in PBS, mounted onto charged microscope slides, dried, and coverslipped with Fluoromount-G medium.

For motor cortex injections, mice were euthanized 13-14 weeks post-injection of α-Syn PFFs. Sections containing the cortex were collected for IHC. Brain sections were stained for α-Syn aggregates (α-Syn phosphorylated on Ser129), excitatory neurons (CAMK2α), inhibitory neurons (GAD67), and PV interneurons. Information regarding primary and secondary antibodies of interest, as well as their corresponding dilution quantities and incubation times, can be found in Tables 1 and 2.

For dorsal striatum injections, mice were euthanized 11-15 weeks post-injection of α-Syn PFFs. Sections containing the dorsal striatum were collected for IHC. Brain sections were stained for α-Syn aggregates (α-Syn phosphorylated on Ser129) and medium spiny neurons (DARPP-32). Information regarding primary and secondary antibodies of interest, as well as their corresponding dilution quantities and incubation times, can be found in Tables 1 and 2.

Fluorescence Microscopy and Image Analysis

We used a Nikon eclipse Ti2 fluorescence microscope to image stained brain sections. We first used a 4x objective to generate a tiled overview image of the entire brain section. Using the Allen Brain atlas as a reference, we manually identified regions of interest and then collected Z stacks (step size=2 μm) at a magnification of 20X. Information regarding fluorescent filter cubes, exposure times, and illumination light intensity for each marker of interest can be found in Table 3. Compiled z-stack images were then deconvolved using Nikon's NIS Elements 2D Blind deconvolution software to remove out-of-plane fluorescence. Information regarding deconvolution parameters for markers of interest can be found in Table 4. Max intensity projection images were then created using Nikon NIS Elements software. ROIs for α-Syn aggregates were identified by setting a pixel intensity threshold of 20,000 to 65,000 and a size range of 50-1000000μm².

For the cortex, in each imaged region, we examined for colocalization of somatic α-Syn aggregates with markers for Camk2α, GAD67, and PV. For the dorsal striatum, we quantified

the colocalization of somatic α-Syn aggregates with MSN subtypes. In order to differentiate between D1 and D2 MSNs, we scored DARPP-32+/tdTomato- cells as D2-MSNs. Cells that were DARPP-32+/tdTomato+ or exclusively tdTomato+ were classified as D1-MSNs.

For each image, we calculated α-Syn aggregate density by dividing the total number of α-Syn aggregates by the area of the brain region of interest (in mm^2). Each α-Syn aggregate was then categorized as either somatic or non-somatic. α-Syn aggregates that colocalized entirely within the outlines of neuronal somata were classified as somatic aggregates. α-Syn pathology that appeared neuritic in morphology or crossed the borders of one or more neuronal somata were classified as non-somatic aggregates. The number of somatic and non-somatic aggregates was then totaled across all images. We then focused on somatic aggregates. For each image, the total number of cells for each cell type colocalizing with somatic α-Syn aggregates was divided by the area of the brain region of interest in which aggregates were quantified.

To estimate the proportion and percentage of each cell type containing somatic α-Syn aggregates, we first estimated the total number of cells of each cell type in our imaged sections. Since it was not possible to count every cell in a large area for very common cell types (CAMK2α+, DARPP-32+, and tdTomato+ cells), we selected a random sub-region of each image, counted all the cells in that region to obtain the density of cells and extrapolated that density of cells to the larger image to obtain an estimate of the total number of cells across the entire image. For cell types that were more sparsely labeled (GAD67 and PV), the total number of cells in each image containing our region of interest was manually counted. For PV we first ran our images through cellpose software under the parameters of a diameter of 55 pixels and model zoo “cyto” before manually checking that all PV+ cells were correctly identified.

Statistical Analysis

Statistical analyses were conducted using Prism (GraphPad). All data is displayed as mean ± SEM. Data was checked for normality, and parametric and non-parametric tests were used as indicated in the associated figure legends. To examine for statistical difference in the proportion of our cell-types we conducted a chi-square test. Our chi-square table consisted of the total quantity of α-Syn+ cells, as well as the value calculated from subtracting the total quantity of α-Syn+ cells from the total estimated number of cells across all image sets for each cell type of interest.

Results

In order to investigate whether there may be a cell-type specific vulnerability for α-Syn aggregate formation, we injected α-Syn PFFs into either the primary motor cortex or dorsolateral striatum. We chose these two regions as these regions are known to exhibit Lewy pathology and are implicated in motor and cognitive impairments in patients with PD. We first wanted to ensure that injection of α-Syn PFFs results in α-Syn pathology in our brain regions of interest. We injected α-Syn PFFs or DPBS into the primary motor cortex of 10-week-old WT C57BL/6J mice (Figure 1), as well the dorsal striatum of 8-10 week-old hemizygous Tg(Drd1a-tdTomato)6Calak/J transgenic mice (Figure 2). WT C57BL/6J mice were transcardially perfused 13-14 weeks post-injection (Figure 1), while hemizygous Tg(Drd1a-tdTomato)6Calak/J transgenic mice were transcardially perfused 11-15 weeks post-injection (Figure 2). We then extracted the brains and performed immunofluorescence staining for pSer129-α-syn on coronal sections to label aggregated α-Syn. In both the cortex and dorsal striatum, we observed significant α-Syn pathology in α-Syn PFF injected mice but not control mice injected with DPBS (Figure 3A-D). We quantified the number of pSer129-α-syn positive particles in each image and calculated the average density of α-Syn pathology. We found that the average density of α-Syn pathology was 73.93 ±19.25 aggregates/mm² (Figure 3E) in the cortex of WT C57BL/6J mice and 245.4 ±48.25 aggregates/mm² in the dorsal striatum of hemizygous Tg(Drd1a-tdTomato)6Calak/J transgenic mice (Figure 3F).

We next sought to determine the specific cell types with which pSer129-α-syn positive particles colocalized. To validate the specificity of our cell type markers, we performed control experiments for some of our antibodies of interest. Based on in situ hybridization data from the Allen brain atlas, GAD67 expression is enriched in the cortex compared to the thalamus[32]. Consistent with this, we found that immunofluorescence staining using our selected GAD67 antibody strongly labeled cells in the cortex but not the thalamus (Figure 4A-4B). Furthermore, in tissue co-stained for GAD67 and Camk2α, we found that GAD67+ and CAMK2α+ cell somas

in the cortex did not colocalize, suggesting that our strategy for immunofluorescence staining is labeling distinct excitatory and inhibitory cell populations (Figure 4G). For the dorsal striatum, we chose the marker DARPP-32 to label MSNs. Based on in situ hybridization data from the Allen brain atlas, DARPP-32 is highly expressed in the striatum but not in the cortex[33]. Using an antibody specific for DARPP-32 to perform immunofluorescence staining, we observed an abundance of DARPP-32+ cells in the dorsal striatum but none in the cortex as expected (Figure 5), confirming the specificity of this antibody.

Using our cell-specific markers, we next sought to assess if there is a cell-type specific vulnerability to α-syn aggregation formation in the cortex. We conducted IF staining for the markers Camk2α, GAD67, and PV, and used pSer129-α-synuclein to label aggregated α-Syn in cortical sections from mice injected with α-Syn PFFs in the primary motor cortex. We first classified pSer129-α-synuclein+ aggregates into somatic or non-somatic categories based on whether the aggregates were restricted to cell somas based on our cell-type markers. Across all quantified images, we found 50 somatic and 585 non-somatic pSer129-α-synuclein+ aggregates (Figure 7A). We then focused on somatic aggregates and found that pSer129-α-synuclein+ aggregates predominantly colocalized with Camk2α+ cells (Figure 6A), with pSer129-α-synuclein aggregates colocalizing with GAD67+ and PV+ cells to a much lower extent (Figure 6B-C). To quantify this, we first calculated the density of cells colocalizing with somatic α-Syn aggregates for each cell type in the cortex. The average density of cells with somatic α-Syn aggregates was 7.42 ± 2.37 cells/mm², 1.37 ± 0.86 cells/mm² and 1.13 ± 0.77 cells/mm² for Camk2α, GAD67, and PV, respectively (Figure 7B). The density of Camk2α cells with somatic α-Syn aggregates was significantly greater than GAD67 or PV cells (Figure 7B). A significant difference was observed between Camk2α and GAD67 (Figure 7B). We then calculated the percentage of each cell type with somatic α-Syn aggregates by dividing the number of cells positive for somatic α-Syn aggregates by the total number of estimated cells in the imaged region and then multiplied our value by 100. We found that the percentage of α-Syn+ cells was

0.64± 0.20 cells/total estimated cells for Camk2α, 3.33 ±1.92 cells/total estimated cells for GAD67, and 1.19 ± 0.96 cells/total estimated cells (Figure 7). While no statistical significance was observed between cell types, a higher percentage mean was seen with GAD67 compared to CAMK2α and PV (Figure 7). We then conducted a chi-square test and observed a statistical significance on the proportion of Camk2α and GAD67 cells across all images from all mice ($p=0.0007$). GAD67 had a higher proportion with inclusions compared to CAMK2α. No statistical significance was seen between the proportion of Camk2α and PV cells with inclusions or GAD67 and PV cells with inclusions.

To investigate if there is a cell-type vulnerability in α-Syn aggregation formation in the dorsal striatum, we next performed IF staining on sections from hemizygous Tg(Drd1a-tdTomato)6Calak/J transgenic mice injected with α-Syn PFFs in the dorsolateral striatum. This strain of mice expresses tdTomato specifically in D1-MSNs. Combined with staining for DARPP-32 to broadly label most MSNs, we differentiated D1- and D2-MSNS by scoring DARPP-32+/tdTomato- cells as D2-MSNs and DARPP-32+/tdTomato+ or DARPP-32-/tdTomato+ cells as D1-MSNs. Staining for pSer129-α-synuclein, we counted 287 somatic and 509 non-somatic α-Syn aggregates across all quantified images (Figure 9A). Somatic pSer129-α-synuclein+ aggregates colocalized with both D1 and D2 MSNs (Figure 8). We next calculated the density of cells with α-Syn aggregates for each cell type and found 48.71 ± 5.77 cells/mm² for D1 MSNs, and 25.59 ± 5.62 cells/mm² for D2 MSNs (Figure 9B). A statistical difference in the density of cells with α-Syn aggregates was observed between D1 and D2 MSNs (Figure 9B). In order to account for potential differences in the number of D1 and D2 MSNs in our imaged regions, we further calculated the proportion of each cell type with somatic α-Syn aggregates by dividing the number of cells positive for somatic α-Syn aggregates by an estimate of the total number of D1 or D2 MSNs in the imaged region. We found that the % of α-Syn+ cells was 1.73± 0.22 cells/total estimated cells for D1-MSNs and 1.16 ± 0.26 cells/total estimated cells for D2 MSNs (Figure 9C). Although D1 MSNs had a greater mean percentage, no significant difference was

observed between D1 and D2 MSNs. (Figure 9). Lastly, we conducted a chi-square test on the proportion of D1- and D2-MSNs across all images from all mice and a statistically significant was observed between D1 and D2 MSNs ($p=0.0028$). D1 MSNs had a higher proportion with inclusions compared to D2 MSNs.

Discussion

In this study, we sought to investigate the hypothesis that there may be a cell-type-specific vulnerability to the formation of pathological α-Syn aggregates. To do so, we injected α-Syn PFFs directly into either the motor cortex or dorsal striatum, two sites implicated in the cardinal motor symptoms of PD. The PFF model has been well characterized and leads to time-dependent, progressive formation of intracellular α-Syn pathology that spreads along anatomically connected regions, recapitulating the pathology seen in patients with PD. However, to date, there have been few studies examining whether specific neuronal sub-populations may be selectively vulnerable to the formation of α-Syn aggregates. In fact, to our knowledge, no study has investigated this question in the dorsal striatum, nor have there been any studies investigating the cell-type specific vulnerability of cortex neurons after α-Syn PFF injection directly into the primary motor cortex. As expected, we found that injection of α-Syn PFFs into either the primary motor cortex or the dorsolateral striatum produced robust α-Syn pathology in both regions (Figure 3). In both the cortex and dorsal striatum, we observed α-Syn pathology that co-localized within the outlines of neuronal somata, as well as other pathology that appeared neuritic in morphology or crossed the borders of one or more neuronal somata (Figure 9). We classified these into somatic and non-somatic aggregates, respectively. We found that non-somatic aggregates significantly outnumbered somatic aggregates in both brain regions. This may be due to the localization and enrichment of α-Syn at pre-synaptic (neuritic) sites and is consistent with other studies suggesting aggregation may occur first at pre-synaptic neuritic sites before appearing in the neuronal soma[34].

We next focused on somatic α-Syn aggregates and quantified the colocalization with cell-type specific markers. In the cortex, somatic α-Syn aggregates were observed to primarily colocalize with excitatory neurons. The density of excitatory neurons (CAMK2α) with somatic α-Syn aggregates was higher than that for inhibitory neurons in general (GAD67), and for PV interneurons. In order to account for the fact that excitatory neurons far outnumber inhibitory

neurons in the cortex, we calculated the percentage of each cell type with somatic α-Syn aggregates and found no statistical difference in the percentage with somatic α-Syn aggregates between excitatory neurons and inhibitory interneurons (GAD67 and PV). In contrast with this finding, through using a chi-square test across all quantified aggregates, we observed a statistical significance between the proportion of Camk2α and GAD67 cells across all images from all mice ($p=0.0007$). A greater proportion of inhibitory interneurons had somatic α-Syn aggregates compared to excitatory neurons. These results suggest that both excitatory and inhibitory cortical neurons are capable of forming α-Syn aggregates, and that there may be an inhibitory interneuron vulnerability for α-Syn aggregate formation. In the dorsal striatum, we observed somatic α-Syn aggregates frequently colocalizing with D1 and D2 MSNs (Figure 8). A statistical significance between the density of D1 and D2-MSNs with α-Syn aggregates was observed (Figure 9). In divergence with this finding, no statistical difference was observed between the percentage of D1 or D2 MSNs with somatic α-Syn aggregates. Through using a chi-square test across all quantified aggregates, we observed a difference in the proportion of D1 and D2 MSN cells across all images from all mice ($p= 0.0028$) (Figure 8). A greater proportion of D1 MSNs had somatic α-Syn aggregates compared to D2 MSNs. This finding suggests that there may be a cell-type vulnerability to α-Syn aggregate formation in D1 MSNs in the dorsolateral striatum after α-Syn PFF injection.

To our knowledge, this study is the first to assess if there is a cell-type-specific vulnerability to the formation of α-syn aggregates in the dorsolateral striatum. In addition, no studies have examined cell-type-specific vulnerability to α-Syn aggregate formation after direct injection of PFFs in the primary motor cortex. However, after injection of PFFs in the dorsal striatum, a study found that α-Syn aggregates primarily colocalize with excitatory neurons in the amygdala and prefrontal cortex[25]. In the pedunculopontine nucleus, α-Syn aggregates were also observed to colocalize preferentially with excitatory cholinergic neurons after α-Syn PFF injection into the pedunculopontine nucleus[18]. While our findings from examining the density of

cells with α-Syn aggregates support the notion that in the cortex, excitatory neurons have a cell-type specific vulnerability for α-Syn aggregate formation, our % of α-Syn+cells and chi-square results do not. Furthermore, our chi-square test findings suggest that there is a cell-type vulnerability for α-Syn aggregate formation in inhibitory interneurons.

While the mechanism underlying this suggested cell-type-specific vulnerability remains unclear, one hypothesis is that it is related to α-Syn expression levels. Expression of α-Syn has been shown to influence regional vulnerability to the spread of α-Syn pathology[35]. Prior research has shown that in the cerebral cortex, endogenous α-Syn is observed to colocalize with synapses labeled by the vesicular glutamate transporter (vGluT), a marker for excitatory neurons[36]. Colocalization was not seen between endogenous α-Syn and GAD+ synapses, a marker for inhibitory neurons[36]. In the cortex α-Syn pathology was observed in excitatory and inhibitory neurons. Furthermore, our results suggest that there may be a cell-type vulnerability for inhibitory interneurons. These findings suggests that there could be other factors besides α-Syn expression levels influencing α-Syn pathology propagation. Prior studies have demonstrated that α-Syn expression is required for α-Syn aggregate formation[37]. This notion leads us to hypothesize that both MSNs express α-Syn, though we are not aware of any studies examining differential expression of α-Syn between these two cell types.

This study has several limitations. Although we validated the specificity of our cell-specific markers (GAD67, CAMK2α, and DARPP-32), the staining pattern is not homogenous and often stains both cell soma and puncta localized to neuritic structures (Figures 4 and 5). This made it challenging to delineate boundaries of neuronal somata in some cases, particularly for GAD67. In the future, using Cre-driver lines to express soluble fluorescent proteins to label neuronal sub-populations, similar to our approach for labeling D1-MSNs, might offer a more robust method for colocalization analysis. This approach might also facilitate the classification of non-somatic α-Syn aggregates, which we were not able to do here. In some cases, particularly for PV interneurons, our sample size was low, and thus our analyses may be underpowered.

The cell-type specific markers we used here were also not comprehensive. In the future, we plan to expand our analysis to include markers for additional subtypes of inhibitory neurons in the cortex (such as somatostatin and vasoactive intestinal peptide interneurons) and cholinergic and GABAergic interneurons in the striatum. To calculate the percentage of specific cell types colocalizing with somatic α-Syn aggregates, we had to estimate the total number of CAMK2α, GAD67, D1-MSNs, and D2-MSNs as detailed in our material and methods section. In the future, an unbiased stereology approach might allow for more precise quantification of the total number of cells in our images. Finally, although the spread of pathology is a characteristic feature of the PFF injection model, here we restricted our analysis to regions directly adjacent to the PFF injection site. In the future, we plan to expand our analysis to investigate anatomically connected regions to investigate the influence that spread has on cell-type specific vulnerability to α-Syn aggregate formation.

In summary, we have found that injection of α-Syn PFFs into the primary motor cortex and dorsolateral striatum induces robust local formation of α-Syn aggregates. Aggregates were preferentially non-somatic, likely reflecting the early aggregation of α-Syn in pre-synaptic and neuritic structures. In the cortex, both excitatory neurons and inhibitory interneurons are vulnerable to α-Syn aggregate formation. Our work suggests that there may be a cell-type vulnerability to α-Syn aggregate formation in inhibitory interneurons in the cortex. In the dorsolateral striatum, D1 and D2 MSNS are both vulnerable to α-Syn aggregate formation. Our findings suggest that D1 MSNs may be vulnerable to α-Syn aggregate formation. Further work is needed to examine if there is a cell-type-specific vulnerability in GABAergic and cholinergic interneurons in the dorsolateral striatum. Together with other work, our findings suggest that α-Syn expression levels may not be the only important factor influencing the formation of α-Syn aggregates. Our findings suggest additional avenues of research into mechanisms of cell-type-specific vulnerability. We hope that such studies may offer new avenues for therapeutic disease modification in PD.

TABLES AND FIGURES

Primary Antibody	Cell Of Interest	Catalog #	Source	Host species/Isotype/ Mono or Polyclonal	Primary Antibody Dilution	Primary Antibody Incubation Time
α-synuclein (phospho S129)	α-Syn Aggregates	ab51253	AbCam	Rabbit/ IgG/Mono	1:1000	72 hours
CAMK2α	Excitatory Neurons	ab22609	AbCam	Mouse/IgG1/Mono	1:500	72 hours
GAD67	Inhibitory interneurons	MAB5406	Millipore	Mouse/IgG2a/Mono	1:250	72 hours
DARPP-32	Medium Spiny Neurons	MAB4230	Novus Biologicals	Rat/IgG2a/Mono	1:500	72 hours

Table 1: Primary antibodies used for immunohistochemistry on brain sections from C57BL/6J and hemizygous Tg(Drd1a-tdTomato)6Calak/J transgenic mice.

Secondary Antibody	Catalog #	Source	Conjugate	Secondary Antibody Dilution	Secondary Antibody Incubation Time	Corresponding Primary Antibody
Goat Anti-Rabbit polyclonal IgG (H+L) Cross-Absorbed	A-11008	Invitrogen	Alexa Fluor 488	1:500	24 hours	α-synuclein (phospho S129)
Goat anti-Mouse Polyclonal IgG1 Cross-Absorbed	A-21240	Invitrogen	Alexa Fluor 647	1:500	24 hours	CAMK2α
Goat anti-Mouse IgG2a Cross-Absorbed	A-21241	Invitrogen	Alexa Fluor 568	1:500	24 hours	GAD67
Mouse Anti-Rat monoclonal IgG2a heavy chain	ab172333	Abcam	Alexa Fluor 647	1:500	24 hours	DARPP-32

Table 2: Secondary antibodies used for immunohistochemistry on brain sections from C57BL/6J and hemizygous Tg(Drd1a-tdTomato)6Calak/J transgenic mice.

Marker of Interest	Fluorescent Filter Cube	Exposure Time	Illumination light Intensity
α-Syn	GFP	250ms	25%
CAMK2α	CY5	200ms	30%
GAD67	RFP	200ms	30%
DARPP-32	CY5	200ms	30%
D1-MSNs	RFP	200ms	30%

Table 3: Fluorescent filter cubes, exposure times, and illumination light intensity for each marker of interest.

Marker	Dimension	Deconvolution Method	Noise Level	Iterations
α-Syn (phospho S129)	2D	Blind	Automatic except images stained with PV were ran with clear as their noise level	20
Camk2α	2D	Blind	Automatic	22
GAD67	2D	Blind	Automatic	9
PV	2D	Blind	Clear	20
DARPP-32	2D	Blind	Clear	20
tdTomato	2D	Blind	Clear	20

Table 4: Deconvolution settings for each marker of interest.

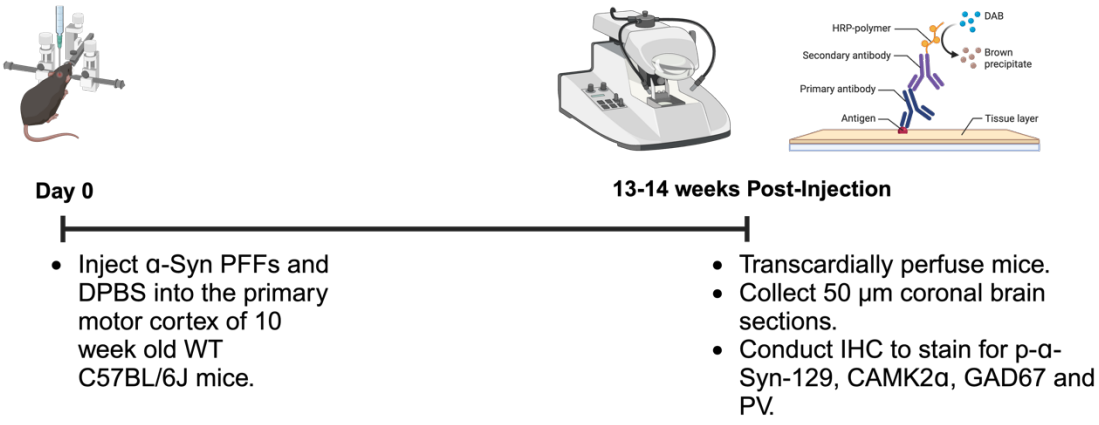

Figure 1: A schematic depicting the experimental protocol for WT C57BL/6J mice.

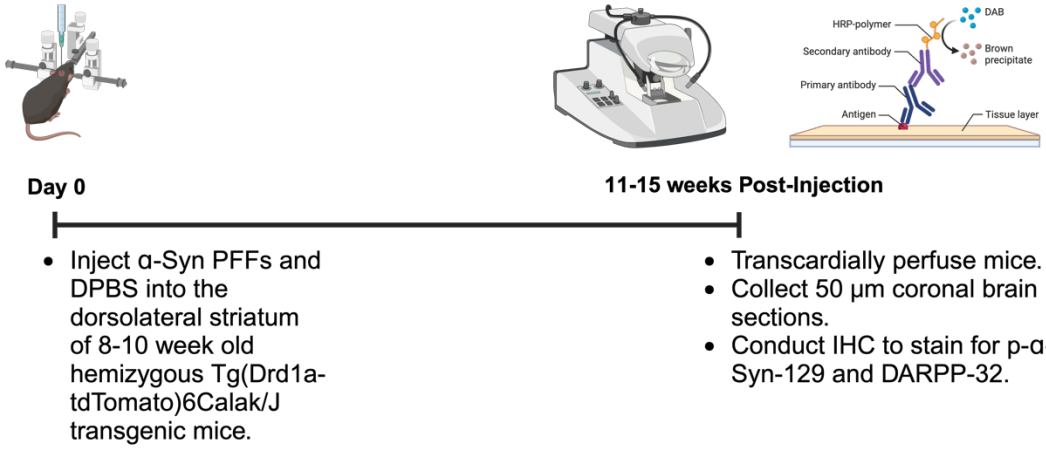

Figure 2: A schematic depicting the experimental protocol for hemizygous Tg(Drd1a-tdTomato)6Calak/J transgenic mice.

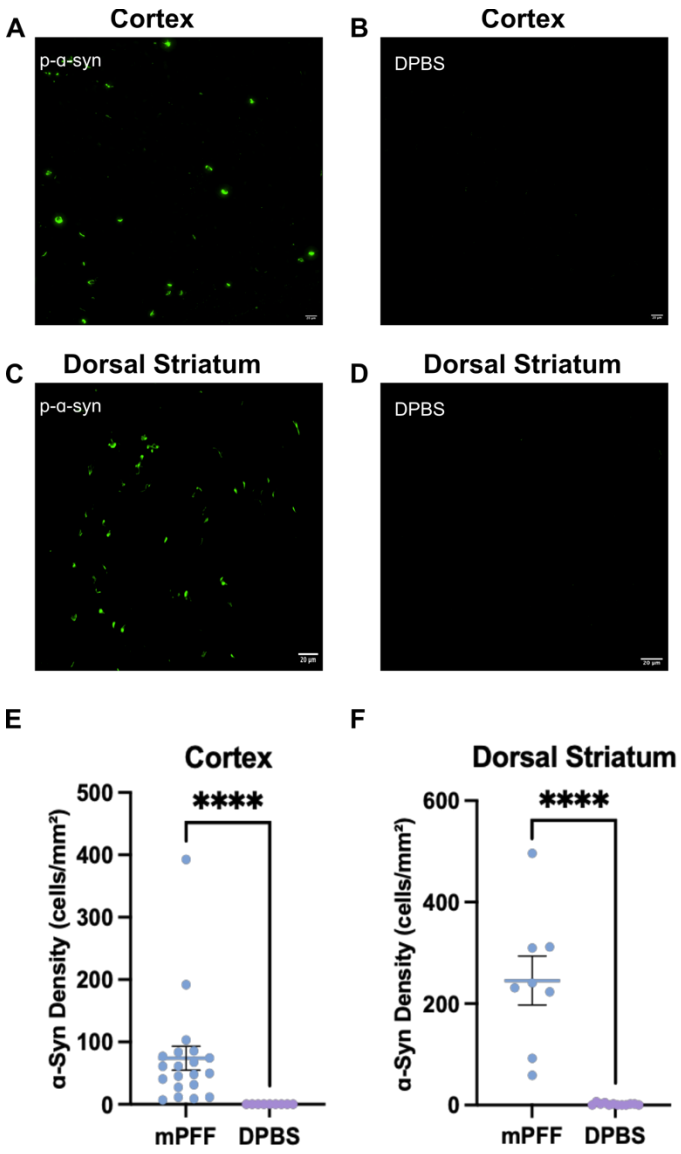

Figure 3: Immunofluorescence and α-Syn phosphorylated on Ser129 density in the dorsal striatum and cortex. (A) Representative image of pSer129-α-synuclein staining in the cortex after α-Syn PFFs were unilaterally injected into the primary motor cortex. **(B)** Representative image of pSer129-α-synuclein staining in the cortex after unilateral control injection of DPBS in the primary motor cortex. **(C)** Representative image of pSer129-α-synuclein in the dorsal striatum after α-Syn PFFs were unilaterally injected into the dorsal striatum. **(D)** Representative image of pSer129-α-synuclein staining in the dorsal striatum after unilateral control injection of DPBS in the dorsal striatum. **(E)** Quantification of the density of pSer129-α-synuclein positive aggregates in the cortex. n=20 images from a total of 4 PFF-injected mice, n=9 images from a total of 2 DPBS-injected mice. *P*<0.0001, Mann-Whitney U test. **(F)** Quantification of the density of pSer129-α-synuclein positive aggregates in the dorsal striatum. n=8 images from a total of 4 PFF-injected mice, n=12 images from a total of 2 DPBS-injected mice. *P*<0.0001, Mann-Whitney U test. Scale bars = 20 μm.

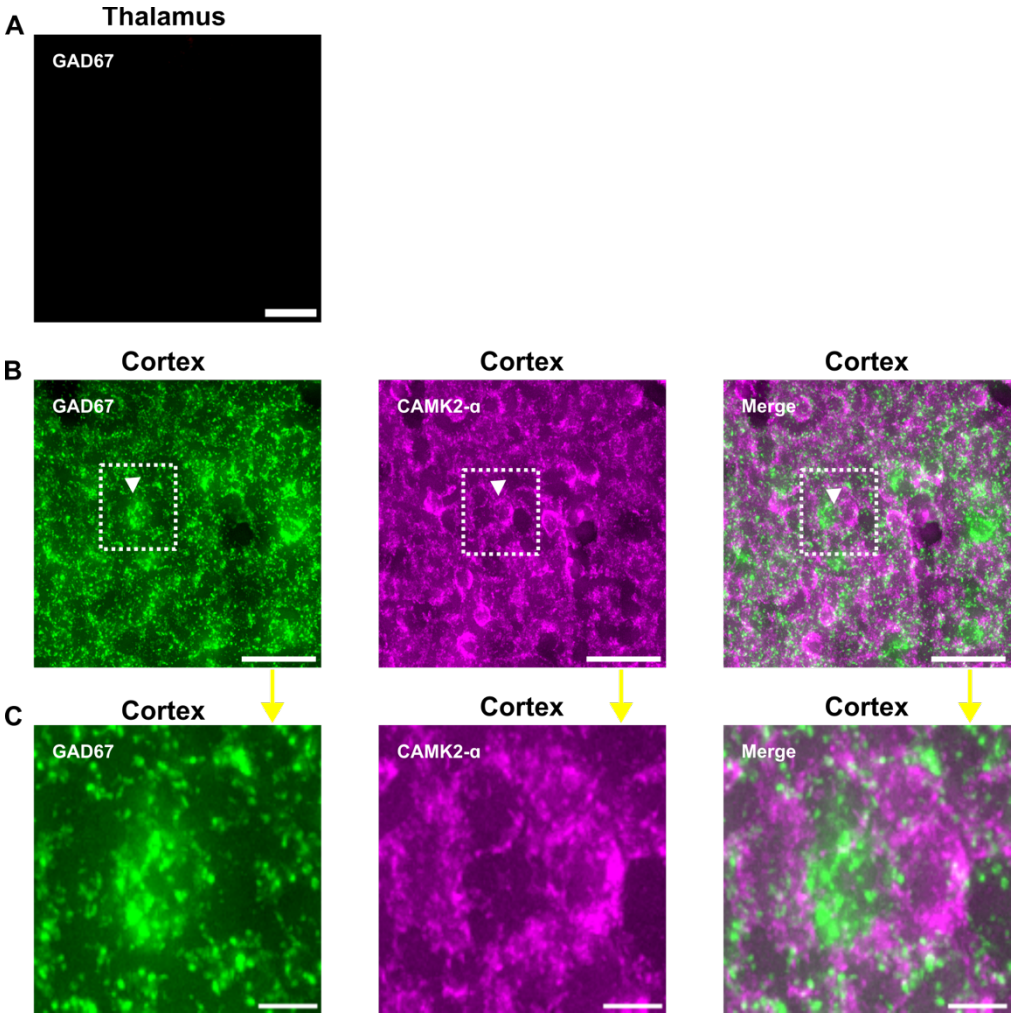

Figure 4: Immunofluorescence staining for GAD67 and CAMK2α in the cortex. (A) Representative image of GAD67 staining in the thalamus, Note the lack of staining, as expected. Scale bar = 50 µm. **(B)** Representative images of GAD67 (left), CAMK2α (middle), and merged image (right) from the cortex. Arrowheads indicate cells of interest highlighted in C. Scale bar = 50 µm. **(C)** Zoomed-in images of individual cells staining positive for GAD67 (left), CAMK2α (middle), and a merged image (right). Note the somas stained for GAD67 and CAMK2a are distinct. Scale bar = 5 µm.

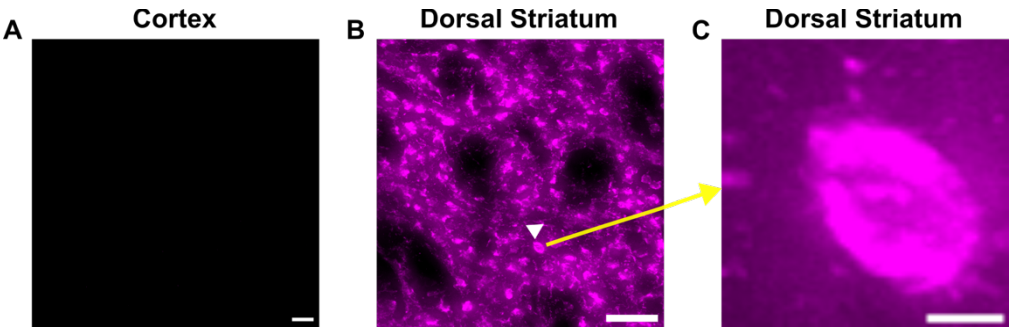

Figure 5: Immunofluorescence staining for DARPP-32 staining in the cortex and dorsal striatum. (A) Representative image of DARPP-32 staining in the cortex. Note the lack of staining, as expected. Scale bar = 50 μm. **(B)** Representative image of DARPP-32 staining in the dorsal striatum. Arrowhead indicates a cell of interest displayed in C. Scale bar = 50 μm. **(C)** Zoomed-in image of a DARPP-32+ cell in the dorsal striatum. Scale bar = 5μm.

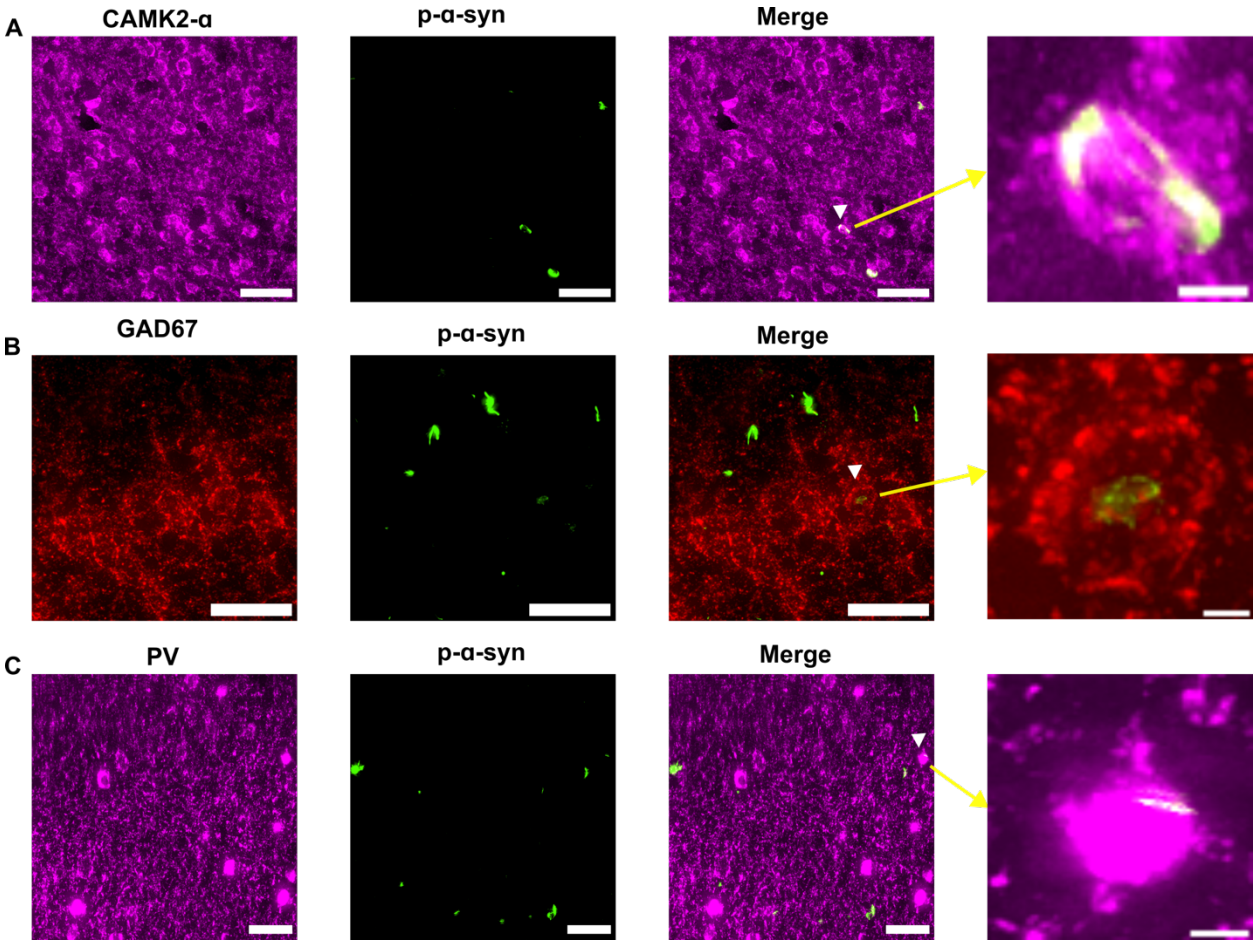

Figure 6: Immunofluorescence colocalization of pSer129-α-synuclein with Camk2α, GAD67, and PV in the cortex. (A) Representative images of CAMK2α (magenta), p-α-Syn-129 (green), and merged image, with arrowhead indicating a CAMK2α+ cell colocalizing with a somatic α-Syn aggregate (zoomed-in image, right panel). **(B)** Representative images of GAD67(red), p-α-Syn-129 (green), and merged image, with arrowhead indicating a GAD67+ cell colocalizing with a somatic α-Syn aggregate (zoomed-in image, right panel). **(C)** Representative images for PV (magenta), p-α-Syn-129 (green), and merged image, with arrowhead indicating a PV+ cell colocalizing with a somatic α-Syn aggregate (zoomed-in image, right panel). Scale bars = 50 μm except for zoomed-in images where scale bar = 5μm.

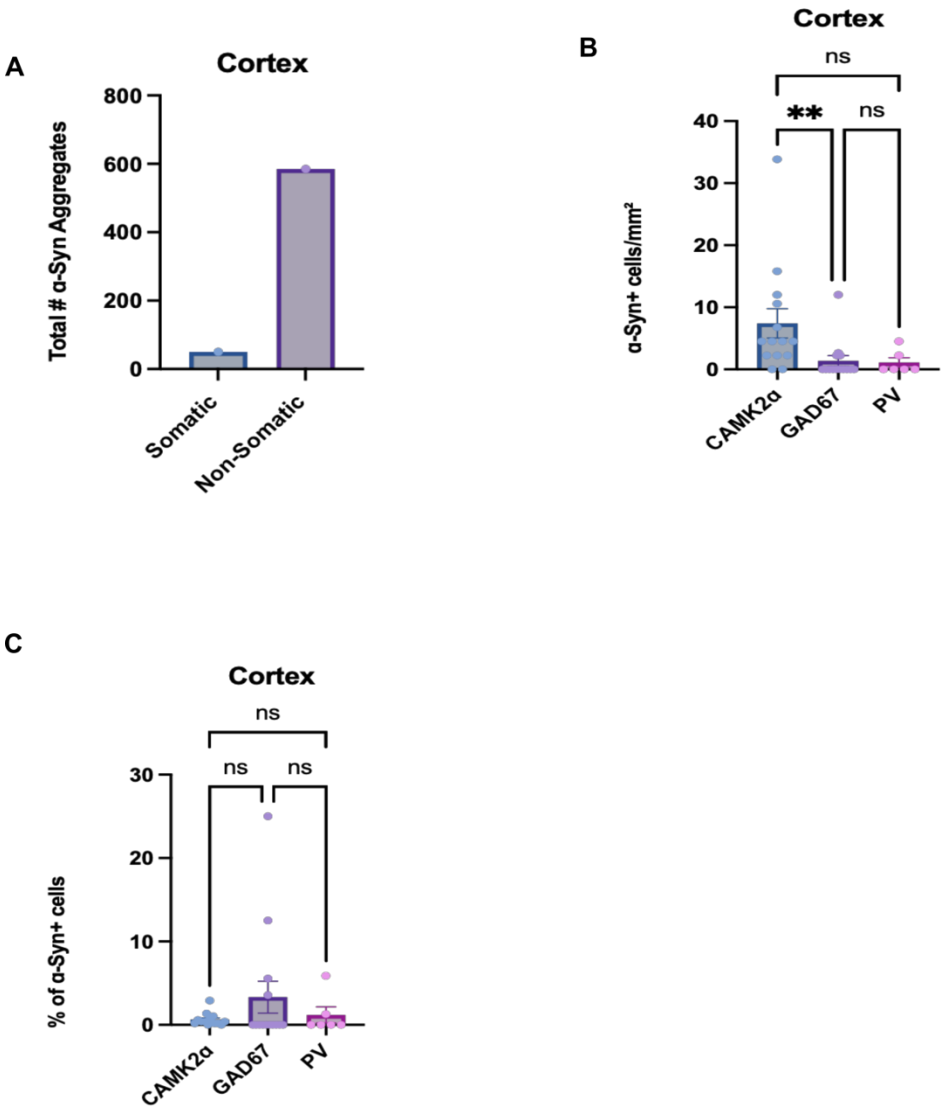

Figure 7: Quantification of α-Syn aggregates in the cortex after unilateral α-Syn PFF injection into the primary motor cortex. (A) The total number of somatic and non-somatic α-syn aggregates quantified in the cortex across 20 images from a total of 4 PFF-injected mice. **(B)** Density of cells in the cortex positive for α-syn aggregates by cell type. n=14 images from a total of 4 mice for Camk2α and GAD67; n=6 images from a total of 2 mice for PV. ***p*=0.0020, Kruskal-Wallis test; ***p*=0.0029, **p*=0.0042 Dunn's multiple comparisons test. **(C)** Percentage of each cell type colocalizing with somatic α-Syn aggregates. n=14 images from a total of 4 mice for Camk2α and GAD67+α-Syn images, n=14 GAD67; +α-Syn images, n=6 images from a total of 2 mice for PV. *p*=0.2651, Kruskal-Wallis test.

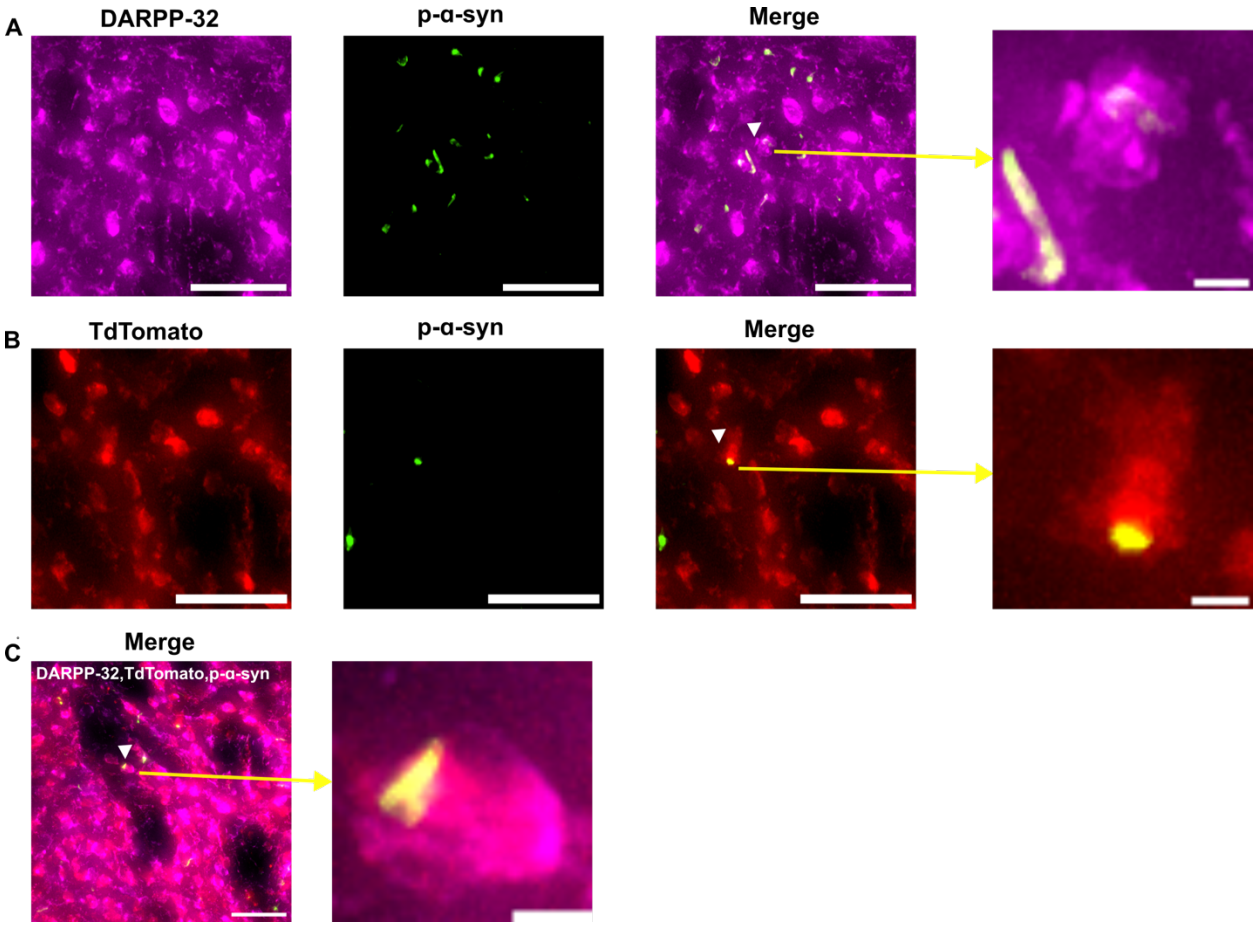

Figure 8: Immunofluorescence colocalization of pSer129-α-synuclein with DARPP-32, and tdTomato in the dorsal striatum. (A) Representative images for DARPP-32 (magenta), pSer129-α-synuclein (green), and a merged image, with arrowhead indicating a DARPP-32 positive cell colocalizing with a somatic α-Syn aggregate (zoomed-in image, right panel). Cells that were DARPP-32+/tdTomato- cells were classified as D2-MSNs, as seen in the merged image. **(B)** Representative images for tdTomato (red), pSer129-α-synuclein (green), and a merged image, with arrowhead indicating a tdTomato positive cell colocalizing with a somatic α-Syn aggregate (zoomed-in image, right panel) **(C)** A merged image of DARPP-32 immunofluorescence, tdTomato fluorescence, and pSer129-α-synuclein immunofluorescence, with arrowhead indicating a DARPP-32/tdTomato double positive cell colocalizing with a somatic α-Syn aggregate (zoomed-in image, right panel). All tdTomato-positive cells were classified as D1-MSNs, while cells that were DARPP-32+/tdTomato- were classified as D2-MSNs. Scale bars = 50 μm (except for zoomed-in images where scale bar = 5μm).

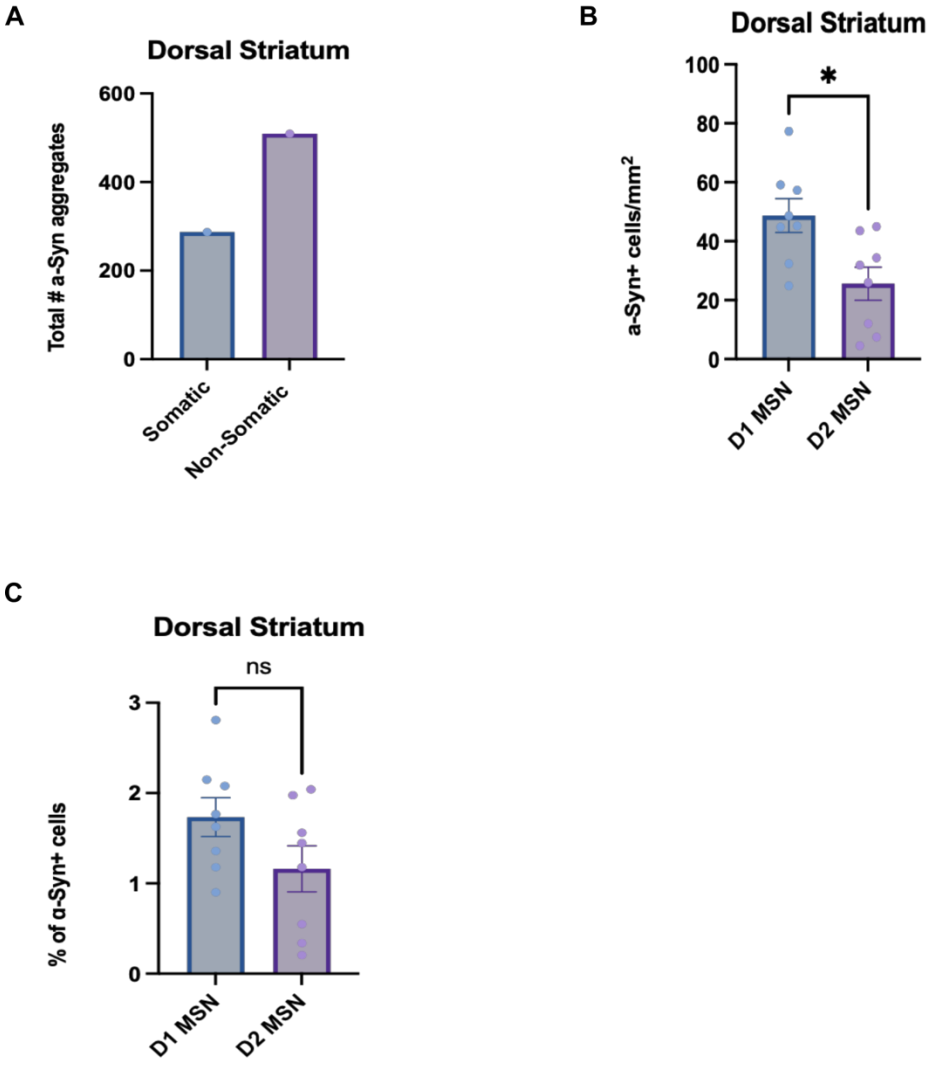

Figure 9: Quantification of α-Syn aggregates in the dorsal striatum after unilateral α-Syn PFF injection into the dorsal striatum. (A) The total number of somatic and non-somatic α-Syn aggregates quantified in the dorsal striatum across 8 images from a total of 4 PFF-injected mice. **(B)** Density of D1 and D2-MSNs colocalizing with somatic α-Syn aggregates. n=8 images from a total of 4 PFF-injected mice. *p=0.0123,unpaired t-test. **(C)** Percentage of D1- and D2-MSNs colocalizing with somatic α-Syn aggregates. n=8 images from a total of 4 PFF-injected mice. ns = not significant, unpaired t-test.

REFERENCES

1. Henderson, M. X., Trojanowski, J. Q. & Lee, V. M.-Y. α-Synuclein pathology in Parkinson's disease and related α-synucleinopathies. *Neuroscience Letters* **709**, 134316 (2019).
2. Pringsheim, T., Jette, N., Frolkis, A. & Steeves, T. D. L. The prevalence of Parkinson's disease: a systematic review and meta-analysis. *Mov Disord* **29**, 1583–1590 (2014).
3. Wooten, G. F. Are men at greater risk for Parkinson's disease than women? *Journal of Neurology, Neurosurgery & Psychiatry* **75**, 637–639 (2004).
4. Tran, J., Anastacio, H. & Bardy, C. Genetic predispositions of Parkinson's disease revealed in patient-derived brain cells. *NPJ Parkinsons Dis* **6**, 8 (2020).
5. Poewe, W. *et al.* Parkinson disease. *Nat Rev Dis Primers* **3**, 17013 (2017).
6. Hely, M. A., Reid, W. G. J., Adena, M. A., Halliday, G. M. & Morris, J. G. L. The Sydney multicenter study of Parkinson's disease: The inevitability of dementia at 20 years: Twenty Year Sydney Parkinson's Study. *Mov. Disord.* **23**, 837–844 (2008).
7. Cerri, S., Mus, L. & Blandini, F. Parkinson's Disease in Women and Men: What's the Difference? *JPD* **9**, 501–515 (2019).
8. Maroteaux, L., Campanelli, J. & Scheller, R. Synuclein: a neuron-specific protein localized to the nucleus and presynaptic nerve terminal. *J. Neurosci.* **8**, 2804–2815 (1988).
9. Burré, J. The Synaptic Function of α-Synuclein. *JPD* **5**, 699–713 (2015).
10. Dauer, W. & Przedborski, S. Parkinson's Disease. *Neuron* **39**, 889–909 (2003).
11. Cookson, M. R. α-Synuclein and neuronal cell death. *Mol Neurodegeneration* **4**, 9 (2009).
12. Luk, K. C. *et al.* Pathological α-Synuclein Transmission Initiates Parkinson-like Neurodegeneration in Nontransgenic Mice. *Science* **338**, 949–953 (2012).
13. Braak, H. *et al.* Staging of brain pathology related to sporadic Parkinson's disease. *Neurobiology of Aging* **24**, 197–211 (2003).
14. Li, J.-Y. *et al.* Lewy bodies in grafted neurons in subjects with Parkinson's disease suggest host-to-graft disease propagation. *Nat Med* **14**, 501–503 (2008).

15. Luk, K. C. *et al.* Exogenous alpha-synuclein fibrils seed the formation of Lewy body-like intracellular inclusions in cultured cells. *Proc Natl Acad Sci U S A* **106**, 20051–20056 (2009).
16. Volpicelli-Daley, L. A., Luk, K. C. & Lee, V. M.-Y. Addition of exogenous α-synuclein preformed fibrils to primary neuronal cultures to seed recruitment of endogenous α-synuclein to Lewy body and Lewy neurite-like aggregates. *Nat Protoc* **9**, 2135–2146 (2014).
17. Rey, N. L. *et al.* Spread of aggregates after olfactory bulb injection of α-synuclein fibrils is associated with early neuronal loss and is reduced long term. *Acta Neuropathol* **135**, 65–83 (2018).
18. Henrich, M. T. *et al.* Determinants of seeding and spreading of α-synuclein pathology in the brain. *Sci. Adv.* **6**, eabc2487 (2020).
19. Paumier, K. L. *et al.* Intrastriatal injection of pre-formed mouse α-synuclein fibrils into rats triggers α-synuclein pathology and bilateral nigrostriatal degeneration. *Neurobiology of Disease* **82**, 185–199 (2015).
20. Shimozawa, A. *et al.* Propagation of pathological α-synuclein in marmoset brain. *acta neuropathol commun* **5**, 12 (2017).
21. Alegre-Abarrategui, J. *et al.* Selective vulnerability in α-synucleinopathies. *Acta Neuropathol* **138**, 681–704 (2019).
22. Tomassy, G. S., Lodato, S., Trayes-Gibson, Z. & Arlotta, P. Development and Regeneration of Projection Neuron Subtypes of the Cerebral Cortex. *Science Progress* **93**, 151–169 (2010).
23. Keaveney, M. K. *et al.* CaMKIIα-Positive Interneurons Identified via a microRNA-Based Viral Gene Targeting Strategy. *J Neurosci* **40**, 9576–9588 (2020).
24. Rudy, B., Fishell, G., Lee, S. & Hjerling-Leffler, J. Three groups of interneurons account for nearly 100% of neocortical GABAergic neurons. *Developmental Neurobiology* **71**, 45–61 (2011).
25. Stoyka, L. E. *et al.* Behavioral defects associated with amygdala and cortical dysfunction in

mice with seeded α-synuclein inclusions. *Neurobiol Dis* **134**, 104708 (2020).

26. Mao, M., Nair, A. & Augustine, G. J. A Novel Type of Neuron Within the Dorsal Striatum. *Front. Neural Circuits* **13**, 32 (2019).
27. Yager, L. M., Garcia, A. F., Wunsch, A. M. & Ferguson, S. M. The ins and outs of the striatum: Role in drug addiction. *Neuroscience* **301**, 529–541 (2015).
28. McGregor, M. M. & Nelson, A. B. Circuit Mechanisms of Parkinson's Disease. *Neuron* **101**, 1042–1056 (2019).
29. Recasens, A. & Dehay, B. Alpha-synuclein spreading in Parkinsonâ€™s disease. *Front. Neuroanat.* **8**, (2014).
30. Ade, K. K., Wan, Y., Chen, M., Gloss, B. & Calakos, N. An Improved BAC Transgenic Fluorescent Reporter Line for Sensitive and Specific Identification of Striatonigral Medium Spiny Neurons. *Front. Syst. Neurosci.* **5**, (2011).
31. Volpicelli-Daley, L. A. *et al.* Exogenous α-Synuclein Fibrils Induce Lewy Body Pathology Leading to Synaptic Dysfunction and Neuron Death. *Neuron* **72**, 57–71 (2011).
32. Allen Institute for Brain Science (2004). Allen Mouse Brain Atlas [Gad1-RP_040324_01_F01-coronal]. Available from mouse.brain-map.org. RRID:SCR_002978 | Primary publication: Lein, E. S. *et al.* Genome-wide atlas of gene expression in the adult mouse brain hi. *Nature* **445**, 168–176 (2007).
33. Allen Institute for Brain Science (2004). Allen Mouse Brain Atlas [Ppp1r1bRP_051121_04_A04 coronal]. Available from mouse.brain-map.org. RRID:SCR_002978 | Primary publication: Lein, E. S. *et al.* Genome-wide atlas of gene expression in the adult mouse brain hi. *Nature* **445**, 168–176 (2007).
34. Kramer, M. L. & Schulz-Schaeffer, W. J. Presynaptic alpha-synuclein aggregates, not Lewy bodies, cause neurodegeneration in dementia with Lewy bodies. *J Neurosci* **27**, 1405–1410 (2007).
35. Henderson, M. X. *et al.* Spread of α-synuclein pathology through the brain connectome is

modulated by selective vulnerability and predicted by network analysis. *Nat Neurosci* **22**, 1248–1257 (2019).

36. Taguchi, K., Watanabe, Y., Tsujimura, A. & Tanaka, M. Brain region-dependent differential expression of alpha-synuclein: α-Synuclein Differential Expression. *J. Comp. Neurol.* **524**, 1236–1258 (2016).
37. Menon, S. *et al.* Viral alpha-synuclein knockdown prevents spreading synucleinopathy. *Brain Communications* **3**, fcab247 (2021).